INTERNATIONAL JOURNAL FOR NUMERICAL METHODS IN FLUIDS, VOL. 14, 25–45 (1992)

A ONE-DIMENSIONAL MOVING GRID SOLUTION FOR THE COUPLED NON-LINEAR EQUATIONS GOVERNING MULTIPHASE FLOW IN POROUS MEDIA. 1: MODEL DEVELOPMENT

AMIR GAMLIEL

Electronic Data Systems Corporation, Environmental Science Department, GM Research Laboratories, Warren, MI 48090-9055, U.S.A.

AND

LINDA M. ABRIOLA

Department of Civil Engineering, The University of Michigan, Ann Arbor, MI 48109, U.S.A.

SUMMARY

A straightforward moving grid finite element method is developed to solve the one-dimensional coupled system of non-linear partial differential equations (PDEs) governing two- and three-phase flow in porous media. The method combines features from a number of self-adaptive grid techniques. These techniques are the equidistribution, the moving grid finite element and the local grid refinement/coarsening methods. Two equidistribution criteria, based on solution gradient and curvature, are employed and nodal distributions are computed iteratively. Using the developed approach, an intermingle-free nodal distribution is guaranteed. The method involves examination of a single representative gradient to facilitate the application of moving grid algorithms to solve a non-linear coupled set of PDEs and includes a feature to limit mass balance error during nodal redistribution. The finite element part of the developed algorithm is verified against an existing finite difference model. A numerical simulation example involving a single-front two-phase flow problem is presented to illustrate model performance. Additional simulation examples are given in Part 2 of this paper. These examples include single and double moving fronts in two- and three-phase flow systems incorporating source/sink terms. Simulation sensitivity to the moving grid parameters is also explored in Part 2.

KEY WORDS Partial differential equations Non-linear equations Coupled system Numerical methods Finite elements Adaptive grid Flow in porous media Groundwater contamination Multiphase flow Immiscible flow

1. INTRODUCTION AND BACKGROUND

Adaptive grid methods have become common tools in the quest for increased efficiency in the numerical solution of partial differential equations (PDEs). This is especially true in computational fluid mechanics, whence came most of the impetus for the development of these techniques.[1] An adaptive grid method is basically a procedure for orderly distribution of discrete points over a physical domain. These points are distributed in such a way that the physical phenomena on the entire domain may be represented at these points with acceptable accuracy and with minimum use of computer resources. Distribution is accomplished by decreasing the

0271–2091/92/010025–21$10.50

Received 13 September 1989
Revised 12 February 1991

spacing between points where large gradients and/or curvatures are involved in the physical phenomenon and increasing the spacing where the gradients and curvatures are small. Adaptive grid techniques may be used for transient problems where the gradients and curvatures may intensify and/or change their locations. These techniques are applicable to domains with regular or irregular, fixed or moving boundaries. Survey works that summarize the basic concepts of the self-adaptive grid are given by Smith,[2] Thompson *et al.*,[3] Thompson and Warsai[4] and Thompson.[1,5,6] In general, these techniques have been developed in order to: (a) reduce the size of the global matrix generated by the primary numerical scheme, in order to save computation time and memory space; (b) resolve oscillations and increase the accuracy of numerical solutions in the neighbourhood of sharp fronts, steep gradients and discontinuities; (c) obtain smooth solutions where the curvature of the function that describes the physical phenomenon is large; and (d) distribute the discrete points over the domain in an orderly fashion so that element connectivities can be easily identified. Four major types of self-adaptive grid approaches may be distinguished: adaptation by equidistribution methods, adaptation by moving grid finite element methods (MFEMs), adaptation by local mesh refinement/coarsening methods and adaptation by variational methods.

The equations describing the immiscible flow of two fluids in a porous medium are a set of strongly coupled non-linear PDEs whose solutions typically exhibit sharp fronts and steep gradients. Finer spatial discretization is often required to limit oscillations and preserve accuracy. Thus these types of problems appear to lend themselves well to solution by adaptive grid methods. Equations governing multiphase flow in porous media represent an important class of problems having applications in oil reservoir simulation, chemical process engineering, unsaturated groundwater flow and non-aqueous phase contaminant transport in groundwater systems.

To date, the use of self-adaptive grid techniques for the solution of multiphase flow problems in porous media has not been fully exploited. This is primarily due to the non-linear and coupled nature of the governing equations. A few works, however, have examined the one-dimensional adaptive grid solution of the Buckley–Leverett equation. This is a single-equation formulation of the two-phase flow problem which was developed to model oil reservoir water flooding and in which the capillary pressure between the fluids is neglected.[7–10] The works of Douglas *et al.*,[7] Gelinas *et al.*[8] and Gruham *et al.*[9] adapted the grid by a moving finite element method. Here the grid moved according to an ordinary differential equation (ODE) generated by differentiation of an equidistribution equation with respect to time. An equidistribution equation is an equation which expresses an equal distribution of some positive weight on each of the discrete elements in the computational domain. The developed ODE was solved simultaneously with the PDE problem. This type of moving grid algorithm was originally proposed in Reference 11. In Reference 10 the Buckley–Leverett equation was solved by a moving boundary technique. In addition to the moving grid works mentioned above, adaptive local grid refinement methods have also been employed for oil reservoir simulation.[12,13] In Reference 12 the use of an implicit pressure, explicit saturation scheme permitted separate treatment of the coupled governing equations. Local refinement was applied to the solution of the saturation equations, which are solved explicitly in the scheme. The influence of capillary pressure was neglected in this approach as with the Buckley–Leverett formulation.

In this paper a straightforward self-adaptive moving grid finite element method is developed for the one-dimensional solution of the *coupled* set of non-linear equations describing immiscible flow. The method contains features of a number of self-adaptive approaches which have been presented previously in the literature. These features are the artificial repulsive force and viscosity which were introduced in References 11 and 14 and the equidistribution function of the gradient

and curvature which was used earlier by a few investigators (e.g. References 15 and 16). These criteria are similar to the first and second norms of the estimate for the error associated with the numerical solution. Adaptations of the equidistribution approach are made herein which facilitate nodal redistribution for coupled sets of non-linear PDEs. This task has been thought to be computationally prohibitive using existing MFEM algorithms (see e.g. References 8 and 17).

Two sets of governing equations are presented in the following pages: one for the immiscible phase flow problem and one for grid redistribution. A moving grid finite element method based on these equations is developed. Unique model features are then discussed. The developed model is verified for a two-phase flow problem and a single-front two-phase flow problem is simulated. Part 2 of this paper details a number of model applications for complicated flow scenarios. A sensitivity analysis of moving grid parameter values is included. In addition, a number of comparisons are made between moving grid and fixed grid solutions, including CPU processing time and memory space.

2. GOVERNING EQUATIONS FOR IMMISCIBLE MULTIPHASE FLOW IN POROUS MEDIA

The general governing equations for immiscible multiphase flow include (a) a continuity equation for each phase, (b) relations between the capillary pressure and the phases' saturation levels, (c) relations between the capillary pressure and the phases' relative permeabilities and (d) the relation among the phases' saturation levels.

The continuity equation

The continuity equation for the α-phase is given as

$$\phi\left(\frac{\partial S_\alpha}{\partial t}+S_\alpha\beta_\alpha\frac{\partial P_\alpha}{\partial t}+S_\alpha\beta_\phi\frac{\partial \bar{P}}{\partial t}\right)=\nabla\cdot\left(\frac{K}{\mu_\alpha}kr_\alpha(\nabla P_\alpha+\rho_\alpha g\nabla z)\right), \tag{1}$$

where g is the gravitational acceleration, $[\mathrm{L}\,\mathrm{T}^{-2}]$, K is the intrinsic permeability, $[\mathrm{L}^2]$, kr_α is the relative permeability of the α-phase, P_α is the pressure of the α-phase, $[\mathrm{M}\,\mathrm{L}^{-1}\mathrm{T}^{-2}]$, $\bar{P}$ is the average pore fluid pressure, $[\mathrm{M}\,\mathrm{L}^{-1}\mathrm{T}^{-2}]$, S_α is the saturation level of the α-phase, z is the length along the vertical co-ordinate, $[\mathrm{L}]$, β_α is the compressibility of the α-phase, $[\mathrm{M}^{-1}\mathrm{L}^4\mathrm{T}^2]$, β_ϕ is the compressibility of the matrix, $[\mathrm{M}^{-1}\mathrm{L}^4\mathrm{T}^2]$, ϕ is the matrix porosity, μ_α is the dynamic viscosity of the α-phase, $[\mathrm{M}\,\mathrm{L}^{-1}\mathrm{T}^{-1}]$, and ρ_α is the density of the α-phase, $[\mathrm{M}\,\mathrm{L}^{-3}]$. It is assumed in (1) that a modified form of Darcy's law controls the flux of the α-phase.

One can simplify equation (1) by lumping the compressibility terms. Here an assumption is made that capillary pressure has a negligible effect on matrix and fluid densities. After lumping these terms, (1) becomes (in the x-direction with an angle θ to the vertical axis)

$$\phi\left(\frac{\partial S_\alpha}{\partial t}+S_\alpha\beta_s\frac{\partial P_\alpha}{\partial t}\right)=\frac{\partial}{\partial x}\left[\frac{K}{\mu_\alpha}kr_\alpha\left(\frac{\partial P_\alpha}{\partial x}+\rho_\alpha g\cos\theta\right)\right], \tag{2}$$

where $\beta_s=\beta_\alpha+\beta_\phi$.

Saturation as a function of capillary pressure

The phase's saturation level is a function of the capillary pressure P_c. An appropriate functional form for this relation was proposed and fitted to data by van Genuchten.[18] This relation is given by

$$S_\alpha=Sr_\alpha+\frac{Ss_\alpha-Sr_\alpha}{[1+(a_{S_\alpha}h_c)^{n_{S_\alpha}}]^{m_{S_\alpha}}}, \tag{3}$$

where a_{s_α} is an empirically determined parameter, h_c is the capillary head between the wetting and non-wetting fluids based on water unit weights ($h_c = -P_c/\rho_w g$), $m_{s_\alpha} = 1 - 1/n_{s_\alpha}$, n_{s_α} is an empirically determined parameter, P_c is the capillary pressure between the fluid phases ($P_{ow} = P_o - P_w$, the capillary pressure between the organic chemical and the water; $P_{wg} = P_w - P_g$, the capillary pressure between the water and the gas), Sr_α is the residual saturation level of the α-phase and Ss_α is the maximum saturation level of the α-phase.

Relations among the phases' saturations

The summation of all the phases' saturations must be unity:

$$\sum_{\alpha=1}^{N_\alpha} S_\alpha = 1 \tag{4}$$

Relative permeability as a function of capillary pressure

The relative permeability is also a function of P_c. A closed-form expression for this function has been derived from the theory developed by Mualem[19] (Reference 18):

$$kr_\alpha = \frac{\{1-(a_{k_\alpha}h_c)^{n_{k_\alpha}-1}[1+(a_{k_\alpha}h_c)^{n_{k_\alpha}}]^{-m_{k_\alpha}}\}^2}{[1+(a_{k_\alpha}h_c)^{n_{k_\alpha}}]^{m_{k_\alpha}/2}}, \tag{5}$$

where a_{k_α} and a_{k_α} are empirically determined parameters and $m_{k_\alpha} = 1 - 1/n_{k_\alpha}$.

Expressions of the form of (3)–(5) have often been applied in the modelling of multiphase flows in groundwater systems[20-22] and will be employed in this paper. For water–trichloroethylene (TCE) two-phase flow, water saturation is calculated by employing (3) and TCE saturation by employing (4). Water relative permeability is estimated by (5) and organic relative permeability is estimated by a modified form of (5),

$$kr_o = a_{k_o}\theta^{1/2}[1-(1-\theta^{m_{k_o}})^{n_{k_o}}]^2, \tag{6}$$

where a_{k_o} is an empirically determined parameter and $\theta = 1-(S_w - Sr_w)/(Ss_w - Sr_w)$. For water–TCE–gas three-phase flow, phase saturations and relative permeabilities are estimated by Stone's[23] method. This method calculates saturations based on the assumptions that organic is the fluid of intermediate wettability in a water–organic–gas pore-filled system and that there is no contact between water and gas. Thus water and total liquid saturations are evaluated by (3) using P_{ow} and P_{wg} respectively as the appropriate capillary pressure, and gas and organic saturations are evaluated by (4). Water relative permeability is evaluated by (5) using $P_c = P_{ow}$. The organic chemical relative permeability is evaluated by weighting its permeability in water–organic and organic–gas (equation (5)) two-phase systems using P_{ow} and P_{og} respectively for P_c. This weighting is accomplished by (a) obtaining the fluids' normalized saturations (equations (7)–(9)) in the water–organic and organic-gas systems, (b) dividing the organic relative permeability in each system by its normalized saturation (equations (10) and (11)) and (c) employing (12) to obtain the weighted organic relative permeability in the three-phase system:

$$S_w^* = \frac{S_w - Sr_w}{1 - Sr_w - Sr_o} \quad \text{for } S_w \geqslant Sr_w, \tag{7}$$

$$S_g^* = \frac{S_g}{1 - Sr_w - Sr_o}, \tag{8}$$

$$S_o^* = \frac{S_o - Sr_o}{1 - Sr_w - Sr_o} \quad \text{for } S_o \geq Sr_o, \tag{9}$$

$$kr^*_{o_{w-o\,system}} = \frac{kr_{o_{w-o\,system}}}{1 - S_w^*}, \tag{10}$$

$$kr^*_{o_{o-g\,system}} = \frac{kr_{o_{o-g\,system}}}{1 - S_g^*}, \tag{11}$$

$$kr_o = S_o^* kr^*_{o_{w-o\,system}} kr^*_{o_{o-g\,system}}. \tag{12}$$

The non-linearity in the flow equations

In this paper the flow of two or three immiscible pore fluid phases will be considered: a water, a non-aqueous organic and a gas (air) phase. It is assumed that the gas pressure remains constant at 1 atm. This is an assumption which has been used by a number of investigators to solve multiphase flow problems in groundwater systems (see e.g. References 24–27). This assumption is employed herein to limit the discussion to two coupled flow equations. Thus equation (2) represents a system of two coupled non-linear PDEs which describes the flow of water, organic chemical and air. This can be easily seen by rewriting (2) explicitly for each phase and incorporating the identity

$$P_o \equiv P_{ow} + P_{wg} + P_g, \tag{13}$$

where the subscripts o, w and g denote the organic, water and gas phases respectively,

$$P_g = 0 \tag{14}$$

and

$$\frac{\partial S_\alpha}{\partial t} \equiv \frac{\partial S_\alpha}{\partial P_{ow}} \frac{\partial P_{ow}}{\partial t} + \frac{\partial S_\alpha}{\partial P_{wg}} \frac{\partial P_{wg}}{\partial t}, \tag{15}$$

since S_α is an explicit function of P_c. Thus the continuity equation for the water phase becomes

$$\phi\left(\frac{\partial S_w}{\partial P_{ow}} \frac{\partial P_{ow}}{\partial t} + \frac{\partial S_w}{\partial P_{wg}} \frac{\partial P_{wg}}{\partial t} + S_w \beta_{s_w} \frac{\partial P_{wg}}{\partial t}\right) = \frac{\partial}{\partial x}\left[K_w\left(\frac{\partial P_{wg}}{\partial x} + \gamma_w \cos\theta\right)\right] \tag{16a}$$

and the continuity equation for the organic phase becomes

$$\phi\left(\frac{\partial S_o}{\partial P_{ow}} \frac{\partial P_{ow}}{\partial t} + \frac{\partial S_o}{\partial P_{wg}} \frac{\partial P_{wg}}{\partial t} + S_o \beta_{s_o} \frac{\partial (P_{ow} + P_{wg})}{\partial t}\right) = \frac{\partial}{\partial x}\left[K_o\left(\frac{\partial (P_{ow} + P_{wg})}{\partial x} + \gamma_o \cos\theta\right)\right], \tag{16b}$$

where

$$K_o = K k_{r_o}/\mu_o, \qquad K_w = K k_{r_w}/\mu_w,$$

$$\beta_{s_o} = \beta_\phi + \beta_o, \qquad \beta_{s_w} = \beta_\phi + \beta_w,$$

$$\gamma_o = \rho_o g, \qquad \gamma_w = \rho_w g.$$

Equations (16a) and (16b) represent a system of two PDEs in two independent unknown pressures P_{ow} and P_{wg}. These equations are coupled through P_{ow}, P_{wg} and the auxiliary equations (3)–(12). Equations (16a) and (16b) are non-linear since all the coefficients, with the exception of β_{s_α}, are functions of the unknowns. Furthermore, the auxiliary functions (3)–(12) generally describe very non-linear expressions relating S_α and kr_α to P_{ow}. Figures 1 and 2 illustrate

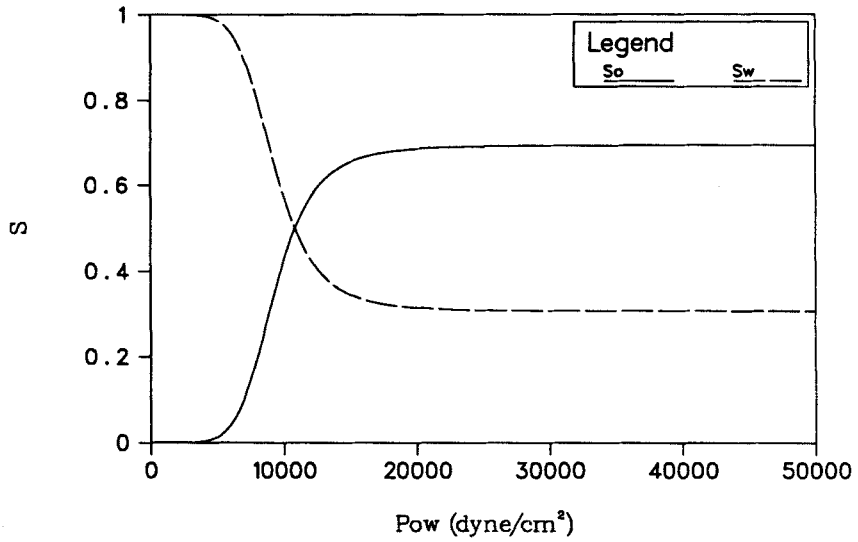

Figure 1. S_o and S_w versus P_{ow} as calculated from Table I for TCE and water

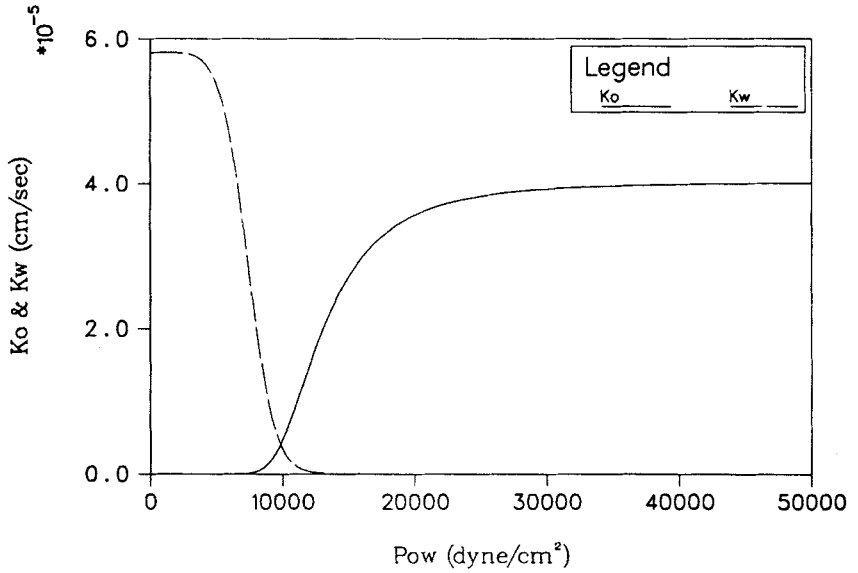

Figure 2. K_o and K_w versus P_{ow} as calculated from Table I for TCE and water

these relations for two-phase flow of TCE and water. These parameter curves were employed in model verification and for the example problem. Note that in Figure 2, K_α is plotted against the capillary pressure, where $K_\alpha = Kkr_\alpha$.

3. GOVERNING EQUATIONS FOR THE SELF-ADAPTIVE MOVING GRID ALGORITHM

In general, multiphase flow problems may involve multiple fronts whose directions of propagation alter during the course of simulation. Mass sources and sinks are also common. As a result,

steep gradients and large curvatures may be present in either of the unknown pressure variables. Thus a moving grid algorithm is sought which is self-adaptive to the changing conditions and which provides for some semi-optimal distribution of nodes to minimize numerical error with respect to both unknown variables and without a great increase in computational cost.

Two equidistribution criteria have been proposed in the literature as estimates of the first and second norms associated with the numerical solution. These are based upon solution gradient and curvature and are especially attractive because they may be readily computed *a priori*. A number of moving grid and mesh refinement algorithms have been based on one or both of these criteria.[7,13,15–17,28,29] The general form of such a criterion can be written as

$$(x_{i+1}-x_i)^q\left(\int_{x_i}^{x_{i+1}}(|\xi(x)|^p+\varepsilon)\,dx\right)^{1/p}=\text{constant}, \tag{17}$$

where x_i is the spatial co-ordinate of node i, $\xi(x)$ is the gradient or curvature function of the unknown, p and q are real constants and ε is a positive rational parameter. The parameter ε was first introduced by Miller and Miller[11] and Miller,[14] who found the use of such a parameter necessary to obtain reasonable nodal distribution solutions based upon some form of (17).

A discrete form of the gradient equidistribution criterion may be obtained by selection of appropriate constants p and q and by letting $\xi \equiv P'$, the gradient in the unknown. Since a linear approximation of the unknown will be obtained with a finite element method employing linear basis functions, the estimate of P' will be constant within an element and (17) becomes

$$(x_{i+1}-x_i)\sqrt{(P_i'^2+\varepsilon_1)}=\text{constant}, \tag{18}$$

where $p=2$ and $q=\frac{1}{2}$ have been chosen to obtain a linear function of the element length and $P_i' \equiv (P_{i+1}-P_i)/(x_{i+1}-x_i)$ is the piecewise constant approximation of the gradient of P in element i.

The parameter ε_1 appearing in (18) is termed an 'artificial repulsive force' in the literature. It is inserted in (18) to overcome the problem of excessive nodal clustering around the largest gradients in the discretized domain and to avoid construction of an ill-conditioned matrix in algorithms which are based on the gradient of the variable when the gradient vanishes or becomes very small. This problem has been identified by a number of investigators through their experience with moving grid finite element methods.[14,16] Note that (18) distributes the grid points more uniformly as ε_1 becomes larger.

Similarly, an equidistribution equation from the criterion to distribute the nodes according to the curvature can be written as

$$(x_{i+1}-x_i)^q\left(\int_{x_i}^{x_{i+1}}(|P''(x)|^p+\varepsilon_2)\,dx\right)^{1/p}=\text{constant}. \tag{19}$$

The above equation incorporates the parameter ε_2, which is commonly called 'artificial viscosity'.[11] This parameter has often been introduced in the self-adaptive moving grid FEMs to provide for an intermingle-free nodal distribution. Its use also avoids the construction of an ill-conditioned matrix in algorithms which are based on the curvature of the variable when the curvature vanishes or becomes very small.

A centred discrete analogue to (19) is sought for a piecewise linear approximation of $P''(x)$. Consider a centred finite difference approximation of P'' at node i, which may be written as

$$\frac{P_i'-P_{i-1}'}{\frac{1}{2}(x_{i+1}-x_{i-1})}, \tag{20a}$$

and similarly at node $i+1$,

$$\frac{P'_{i+1}-P'_i}{\frac{1}{2}(x_{i+2}-x_i)}. \tag{20b}$$

Approximation of P'' by both (20a) and (20b) may be accomplished by weighting these expressions linearly. Substitution of a weighted approximation for P'' in (19) yields

$$B_1(x_{i+1}-x_{i-1})^q\left(\int_{x_{i-1}}^{x_{i+1}}(|P''(x)|^p+\varepsilon_2)\,dx\right)^{1/p}+B_2(x_{i+2}-x_i)^q\left(\int_{x_i}^{x_{i+2}}(|P''(x)|^p+\varepsilon_2)\,dx\right)^{1/p}$$
$$=\text{constant}, \tag{21}$$

where B_1 and B_2 are arbitrary curvature-weighting parameters which can be specified by the user. Sensitivity analysis for the values of these parameters is given in Part 2 of this paper for the problem of immiscible flow in porous media. Equation (21) now becomes

$$(x_{i+1}-x_{i-1})B_1\sqrt{[(P'_i-P'_{i-1})^2+\varepsilon_2]}+(x_{i+2}-x_i)B_2\sqrt{[(P'_{i+1}-P'_i)^2+\varepsilon_2]}=\text{constant}, \tag{22}$$

with $p=2$ and $q=\frac{3}{2}$ chosen to obtain a linear function of the element length.

The gradient (18) and curvature (22) criteria may be combined to yield

$$(x_{i+1}-x_i)\sqrt{(P'^2_i+\varepsilon_1)}+(x_{i+1}-x_{i-1})B_1\sqrt{[(P'_i-P'_{i-1})^2+\varepsilon_2]}$$
$$+(x_{i+2}-x_i)B_2\sqrt{[(P'_{i+1}-P'_i)^2+\varepsilon_2]}=f_i(x_{i-1},x_i,x_{i+1},x_{i+2}), \tag{23}$$

where

$$f_i(x_{i-1},x_i,x_{i+1},x_{i+2})=\text{constant}.$$

Since $f_{i-1}-f_i=0$, (23) leads to the following set of algebraic equations for the nodal distribution:

$$x_1=x(0), \tag{24a}$$

$$f_{i-1}-f_i=0 \quad \text{for } i=2,\ldots,n-1, \tag{24b}$$

$$x_n=x(n), \tag{24c}$$

where the explicit form of (24b) is

$$\begin{aligned}
&x_{i-2}\{-B_1\sqrt{[(P'_{i-1}-P'_{i-2})^2+\varepsilon_2]}\}\\
&+x_{i-1}\{-\sqrt{(P'^2_{i-1}+\varepsilon_1)}+(B_1-B_2)\sqrt{[P'_i-P'_{i-1})^2+\varepsilon_2]}\}\\
&+x_i\{\sqrt{(P'^2_{i-1}+\varepsilon_1)}+\sqrt{(P'^2_i+\varepsilon_1)}+B_1\sqrt{[(P'_{i-1}-P'_{i-2})^2+\varepsilon_2]}+B_2\sqrt{[(P'_{i+1}-P'_i)^2+\varepsilon_2]}\}\\
&+x_{i+1}\{-\sqrt{(P'^2_i+\varepsilon_1)}+(B_2-B_1)\sqrt{[(P'_i-P'_{i-1})^2+\varepsilon_2]}\}\\
&+x_{i+2}\{-B_2\sqrt{[(P'_{i+1}-P'_i)^2+\varepsilon_2]}\}=0.
\end{aligned} \tag{24d}$$

The algebraic equations (24) are employed to determine nodal locations in the moving grid algorithm discussed in the next section. These equations are used in place of more complicated ODEs which can also be developed from equidistribution criteria (17) by differentiating these criteria with respect to time. Such ODEs have been employed in moving grid finite element algorithms in order to solve for both the unknown variable and nodal locations in problems involving a *single* PDE (e.g. References 7, 8, 11, 13, 14, 16, 17 and 28). For problems involving coupled sets of PDEs, however, a *set* of ODEs which describe the nodal locations will result. This set of ODEs forms a multi-objective problem for the nodal locations since the solution of (24) is different for each variable gradient. The solution of such a multi-objective problem is complicated

and time-consuming and an algorithm to solve it simultaneously with a coupled PDE problem is practically unmanageable.[8] Alternatively, the value of a single representative gradient may be calculated *a priori* to the solution of (24) to facilitate the application of an adaptive grid algorithm in the solution of a coupled set of non-linear PDEs. Thus it is proposed to solve (24) in a iterative manner coupled with the finite element algorithm.

It should be noted that an intermingle-free solution is guaranteed in the solution of the set (24) when $B_1 = B_2$, even if the artificial viscosity ε_2 is neglected. This may be demonstrated by the application of the *minimax principle of algebra* (e.g. References 30 and 31). The principle can be applied because the main diagonal is positive, all the off-diagonal terms are negative and the main diagonal is equal to the negative sum of the off-diagonal terms. Here an intermingle-free solution is defined as a solution for which $x_{i-1} < x_i$. A solution in which the nodes intermingle implies that $x_{i-1} \geqslant x_i$ for some nodes and this would result in an unstable numerical algorithm.

4. THE MOVING GRID FINITE ELEMENT ALGORITHM

A modified moving grid finite element method (MGFEM) is now developed which is composed of two basic parts: the finite element algorithm which solves the non-linear coupled set of PDEs and the moving grid algorithm which adapts the grid to the physical conditions in the domain. The finite element algorithm may be any finite element algorithm that can solve the PDEs. The algorithm used in this paper to solve the PDEs which govern multiphase flow in porous media is based on a time-implicit standard Galerkin FEM with linear basis functions and a simple iterative (Picard) procedure. In this algorithm the dependent primary variables P_{wg} and P_{ow} and the non-linear coefficients (secondary variables) K_α, S_α, $\partial S_\alpha/\partial P_{ow}$, and $\partial S_\alpha/\partial P_{wg}$ are approximated with piecewise linear functions. The non-linear coefficients are approximated implicitly by substituting the solution of the dependent variables from the previous iteration into the auxiliary functions (3)–(12). The approximations of the non-linear coefficients are then used to calculate the mass and stiffness matrices for the next iteration. The model calculates the saturation derivatives $\partial S_\alpha/\partial P_{ow}$ and $\partial S_\alpha/\partial P_{wg}$ by a finite element analogue to the well known finite difference chord slope method.[32] This analogue is discussed by Gamliel[33] and had been employed to improve the mass conservation properties of the numerical scheme. The Picard iteration technique is used because of its simplicity, and the iterations proceed until the maximum of the absolute deviation of any new pressure solution from a previous one is less than a small given value δ_1. A more efficient iterative technique could easily be accommodated. Evaluation of the matrix solver efficiency, however, is not a part of this work.

The moving grid adaptation in the MGFEM is accomplished by solution of the set (24). These algebraic equations are solved iteratively with the discretized PDEs. Using this approach, nodal positions can be calculated with various frequencies: every iteration within the non-linear solution process, every time step or every few time steps. In addition, nodal distribution may be performed any time when the absolute deviation of (24d) from zero is greater than some positive value δ_2. The adaptation frequency is then controlled by selecting an appropriate δ_2. The appropriate adaptation frequency was found to vary with the problem under consideration, as discussed in Part 2 of this paper. Once new nodal positions have been computed, solution values at these positions are obtained by interpolation using the model basis functions. All nodal parameters are then evaluated, element lengths are updated and the finite element solution proceeds. The entire solution procedure is summarized in Figure 3.

It must be emphasized that the computation time is greatly reduced by decoupling of the PDE and nodal redistribution problems. If there are k PDEs, one equidistribution equation and n discrete nodes, two matrix problems of size $kn \times kn$ and $n \times n$ are thus solved in place of one

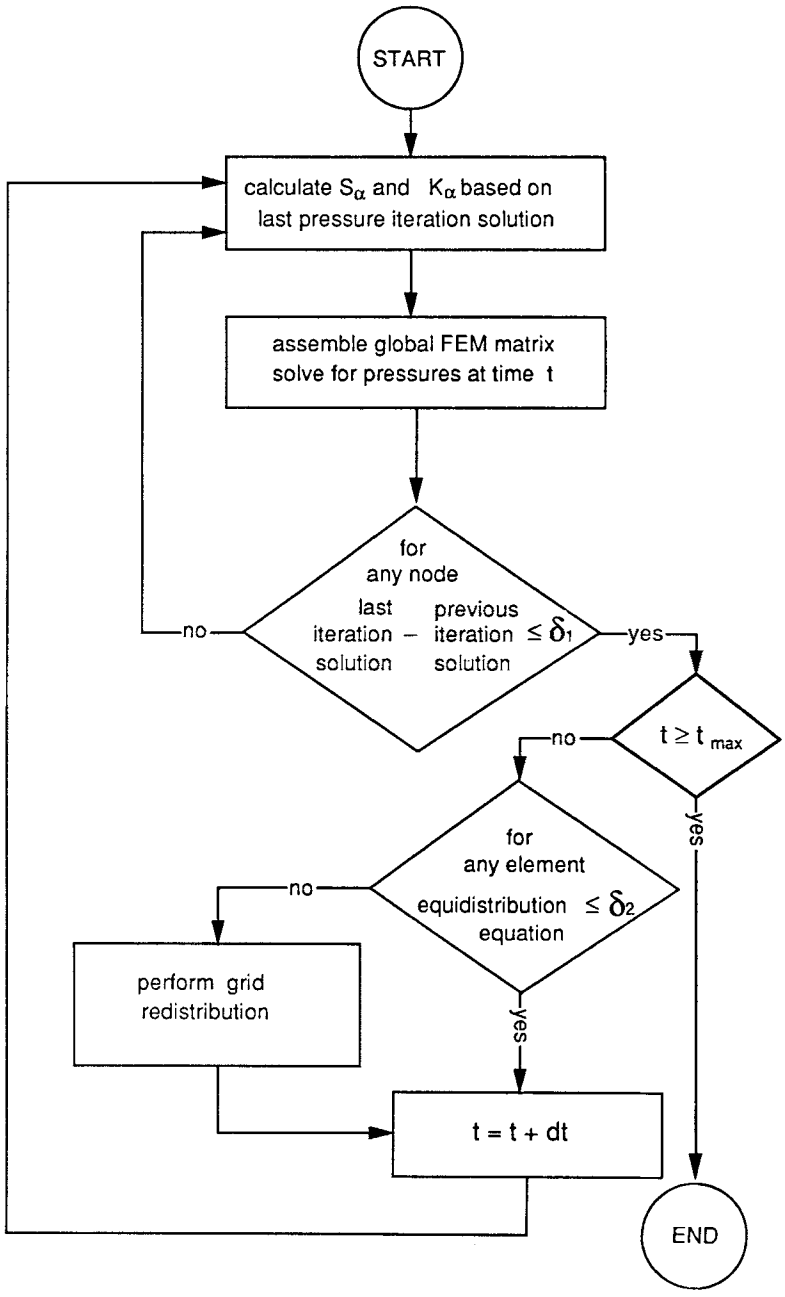

Figure 3. Algorithm flow chart

$(k+1)n \times (k+1)n$ matrix problem with a larger bandwidth. The utility of a non-simultaneous approach for grid adaptivity is also supported by Benner *et al.*,[28] who compared the performance of simultaneous (with the solution of the FEM) and non-simultaneous (after every time step) grid adaptation using an equidistribution criterion similar to (22). In this comparison the difference

between the solutions was found to be negligible and grid adaptation after each time step reduced the computation time by 50%.

The way in which the gradient P'_i in (24) is assigned must be addressed, since it is not obvious how to assign a single representative gradient for a node in a problem with multiple dependent variables. A reasonable representative gradient from the nodal distribution point of view could be the largest gradient among all the variable gradients at each node. That is, at a given node the moving grid algorithm may select the gradient of one variable and at another node it may choose the gradient of another variable. It should be noted that with such a scheme, gradient scaling may prove necessary before choosing the largest gradient for problems with different orders of magnitude in the unknown variables and where grid adaptation with respect to the variable with the smallest gradient is also of interest. Such scaling was not required for the simulations presented in this work. The above approach for selecting the gradient should give a good grid adjustment even for a very complicated domain with several fronts, sources and sinks. In addition, this method of selecting the gradient can adjust the grid for changes in the strength of the sources or the direction of front propagation. The gradient of one variable may be selected for simple problems where only one front is observed, advancing in one direction. Using this approach, the largest gradient among P_{ow} and P_{wg} should be selected for the general problem of organic–water two-phase flow in porous media, and the largest capillary pressure gradient should be assigned for a multiphase flow problem in porous media which involves other fluid phases. The gradient P'_i is the linear approximation of the slope of P_{ow} or P_{wg} in element i, e.g. $|P_{ow,i+1}-P_{ow,i}|/(x_{i+1}-x_i)$ or $|P_{wg,i+1}-P_{wg,i}|/(x_{i+1}-x_i)$. This gradient approximation is consistent with the definition of P'_i in (18).

It should be emphasized that assigning a single representative gradient for each node facilitates the utilization of moving grid algorithms to solve non-linear coupled sets of PDEs. This approach eliminates the need to formulate a few equidistribution equations for each node (one for each variable) and to solve these equations with some non-linear optimization code. Solution with a non-linear optimization code would be required for such problems because different nodal distributions may be produced for each variable. Note that the method of calculating P'_i described above requires a solution for the PDE problem before any grid adaptation. Thus simultaneous solution of the PDEs and the grid is prohibited.

Application of (24) for nodal distribution requires the specification of a number of parameters, i.e. B_1, B_2, ε_1 and ε_2. Guidelines for the selection of these parameters have been developed through numerical experimentation on a number of multiphase flow problems and are discussed in Part 2 of this paper. Specification of a non-zero value for ε_2 was found to be unnecessary in all scenarios examined.

Another important issue is the evaluation of the variables at the new nodal positions after redistribution. This is a significant issue since the evaluation must be consistent with the basic finite element algorithm and must provide for conservation of mass of each phase within the domain. On the basis of these two criteria, it is recommended to evaluate the pressures at the new nodal locations by assuming a linear pressure distribution within each element, since linear interpolation functions are used to approximate pressures in the finite element algorithm, in which pressures are the primary variables. The dependent variables S_α and K_α should then be evaluated using the auxiliary functions (3)–(12) to make these variables consistent with the pressures. Numerical experimentation, however, revealed that this method of evaluation may cause an error in the total mass of each phase within the domain, particularly for problems involving multiple fronts or other local minima/maxima. This problem arises because (3) expresses the saturation as a non-linear function of the capillary pressures. The resultant mass error is illustrated in Figure 4(a), where the symbol '○' represents an initial nodal distribution

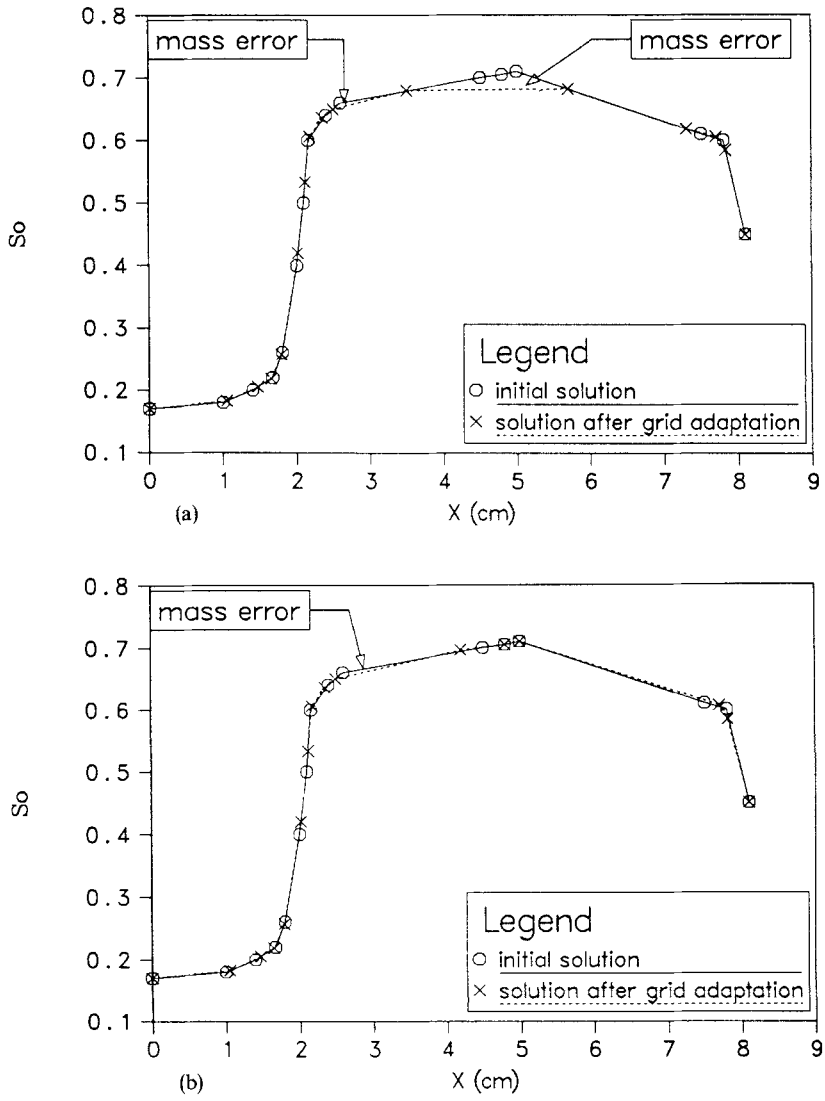

Figure 4. Mass error caused by nodal redistribution (a) without fixing local maximum node and (b) with fixing of local maximum node

and the symbol '×' represents nodes after redistribution. To overcome this problem, saturation could be evaluated at the new nodal locations by linear interpolation and then the pressures could be obtained from the saturations. Such an approach, however, is inconsistent with the numerical scheme, because pressures are the primary variables, and may result in an unstable solution, as has been observed by the authors.

Instead, it is recommended to calculate the pressures by linear interpolation, to compute the saturations from the pressures by (3) and to fix the location of nodes with local maxima or minima in any of the unknown pressures at the time of redistribution. This procedure is designed to assign pressures and saturations at the new nodal positions in a fashion consistent with the numerical

algorithm and to reduce phase mass balance errors to a very negligible value. Momentarily fixing the location of the nodes of local maxima or minima in the pressures means that a test must be performed before each nodal redistribution operation to locate these nodes and that these nodes are to be kept fixed during this redistribution. A local maximum or minimum with respect to a specific pressure is detected in the programme simply by comparing the value of each pressure to the pressure at the neighbouring nodes. If the pressure at a node is lower than the pressure at the two neighbouring nodes, then that node is considered to have a local minimum with respect to the given pressure. An example of fixing a node with a local maximum in P_{ow} is given in Figure 4(b). This example shows the elimination of the error produced in the organic mass about the node having maximum organic chemical saturation. The nodes that are fixed during one redistribution operation may be moved during another redistribution operation, when local minima or maxima in the pressure solution shift to other nodes. In addition, this redistribution scheme solves the problem of maintaining a node in the location of a sink/source point and facilitates the division of

Table I. Soil and fluid parameters used in simulations (after Abriola[20])

Characteristic	Value	Units
g	980.616	$cm\,s^{-2}$
ϕ	0·36	
K	$5{\cdot}2831 \times 10^{-7}$	cm^2
β_ϕ	$2{\cdot}0 \times 10^{-10}$	$cm^2\,dyn^{-1}$
γ_o	1437·28871	$g\,cm^{-2}\,s^{-2}$
μ_o	$5{\cdot}8 \times 10^{-3}$	Poise
β_o	0	
γ_w	980·465	$g\,cm^{-2}\,s^{-2}$
μ_w	0·01	Poise
β_w	$4{\cdot}531 \times 10^{-11}$	$cm^2\,dyn^{-1}$
Water–TCE simulation		
Sr_w	0·306	
Ss_w	0·9998	
a_{s_w}	0·11	cm^{-1}
n_{s_w}	6·50	
a_{k_w}	0·108	cm^{-1}
n_{k_w}	6·60	
a_{k_o}	0·40	
Water–TCE–gas simulation		
Sr_w	0·170	
Ss_w	1·000	
Sr_o	0·170	
Ss_o	1·000	
a_{s_w}	0·1043	cm^{-1}
n_{s_w}	4·690	
$a_{s_{\text{total liquids}}}$	0·0624	cm^{-1}
$a_{s_{\text{total liquids}}}$	8·6050	
a_{k_w}	0·108	cm^{-1}
$n_{k_w}^{w-o\text{ system}}$	0·8560	
$n_{k_w}^{w-g\text{ system}}$	0·8838	
$n_{k_o}^{w-o\text{ system}}$	0·6320	
$n_{k_o}^{o-g\text{ system}}$	0·6216	

the domain into independent segments. These independent segments generate smaller matrix problems out of (24) and in turn the computation time is reduced.

The finite element algorithm used herein was verified against a finite difference solution for problems involving two- and three-phase flow of water and TCE in a 19 cm soil column. The verification of the FEM algorithm outlined above was required because this FEM scheme is the basis for the MGFEM model and is also used as the fixed grid FEM (FGFEM) model. The finite difference model used for model verification is presented in References 24 and 25. This finite difference simulator solves two- or three-phase flow problems of the form (16) with or without interphase mass exchange. The governing PDEs are approximated in the finite difference model with a fully implicit, central difference formulation. The resulting system of non-linear algebraic equations is solved by a Newton–Raphson iterative scheme. Simulation parameters for the FEM verification example are given in Table I. Note that both the FDM and FEM algorithms calculate the TCE saturation and relative permeability by the same methods.

The results of both algorithms for the same nodal spacing and time step size are almost identical for the simulated examples (Figures 5 and 6). Figure 5 shows a comparison between the FEM and the FDM at different times for water displacement by TCE in a two-phase flow regime. Figure 6 compares the solutions of a three-phase flow problem involving gas displacement by TCE. Both simulations were conducted for a horizontal soil column under constant pressure boundary conditions. The initial and boundary conditions for these problems are specified in Table II. Figure 5 also shows finite element simulation comparisons using nodal spacings of 1 cm and 1 mm. A 1 mm nodal spacing was observed to give a smooth sharp front solution with minimal numerical dispersion. Decreasing the nodal spacing further did not visibly improve the solution. Thus solutions based on a 1 mm element length were selected to be used as a basis for the error analysis in subsequent simulations. This was required since analytical solutions are not available for these problems.

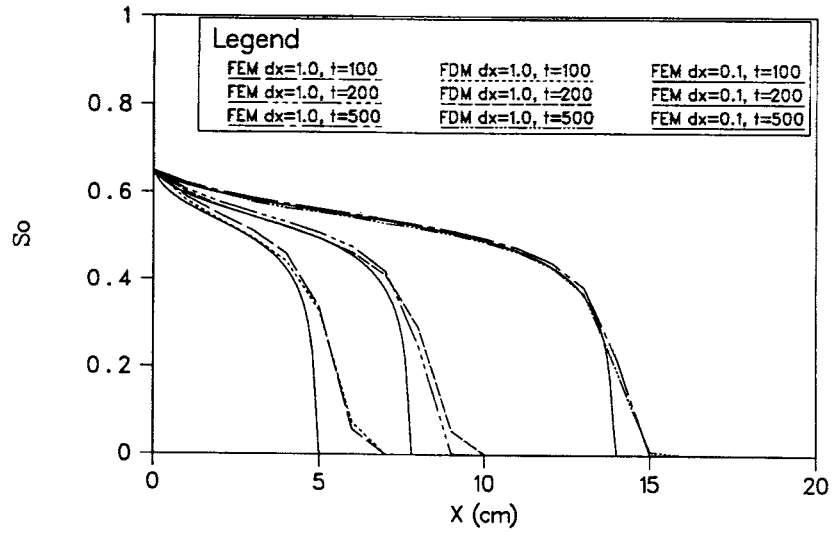

Figure 5. Comparison between the S_o solutions of standard Galerkin FEM and Abriola's FDM in TCE–water two-phase flow simulations

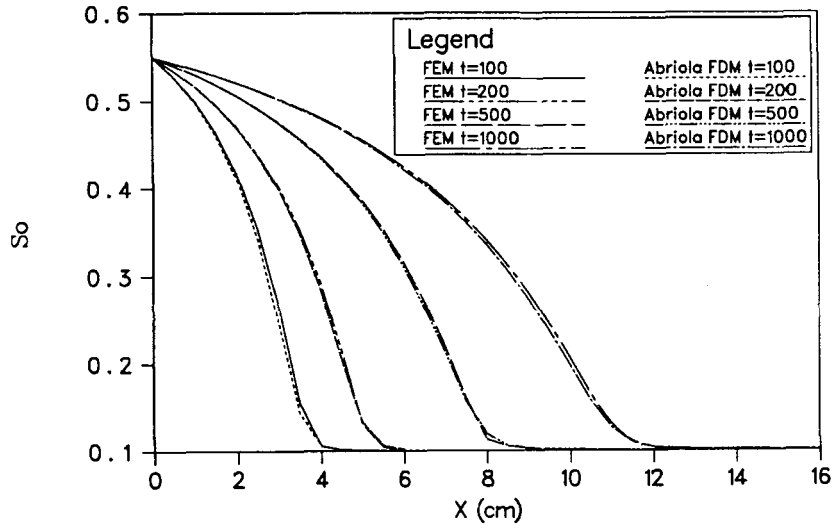

Figure 6. Comparison between the S_o solutions of standard Galerkin FEM ($\Delta x = 0{\cdot}5$ cm) and Abriola's FDM for TCE–water–gas three-phase flow simulation

Table II. Initial and boundary conditions for the problems discussed in this paper

	P_{wg} (dyn cm^{-2})	P_{ow} (dyn cm^{-2})
Two-phase flow verification problem		
Initial conditions	1000	0
Upstream boundary conditions	1000	14610
Downstream boundary conditions	1000	No flux
Three-phase flow verification problem		
Initial conditions	−20135	15210
Upstream boundary conditions	−16853	15210
Downstream boundary conditions	−20135	15210
Simulation example		
Initial conditions	1000	0
Upstream boundary conditions	5900	9710
Downstream boundary conditions	1000	0

5. SIMULATION EXAMPLE

An example of the application of the MGFEM to a two-phase flow problem is given in Figures 7 and 8. Here TCE displaces water in a horizontal soil column. This problem involves a single displacement front. More complicated scenarios are examined in Part 2 of this paper. Results of this simulation were used as initial conditions for a subsequent, multiple-front simulation. The initial and boundary conditions for this problem are specified in Table II. The moving grid

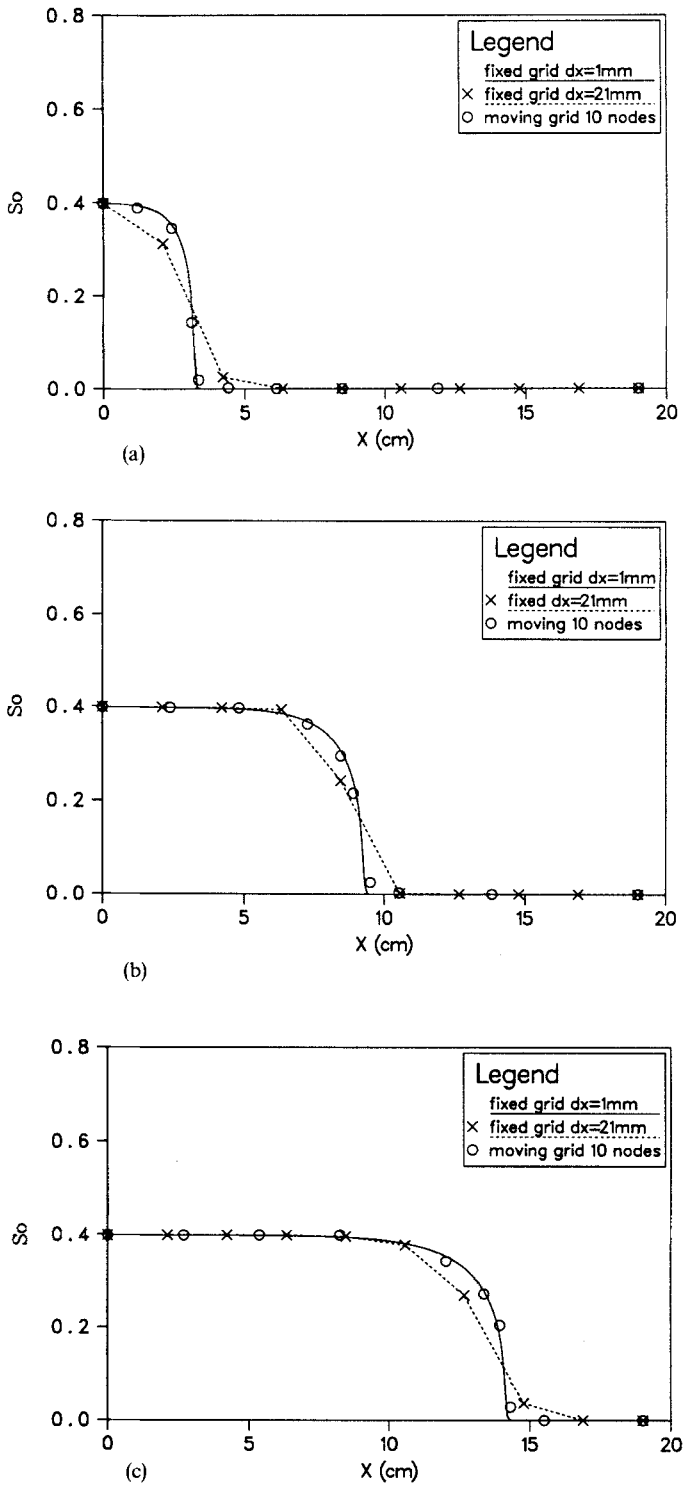

Figure 7. S_o simulation results of TCE–water horizontal single-front flow after (a) 100 s, (b) 500 s and (c) 1000 s

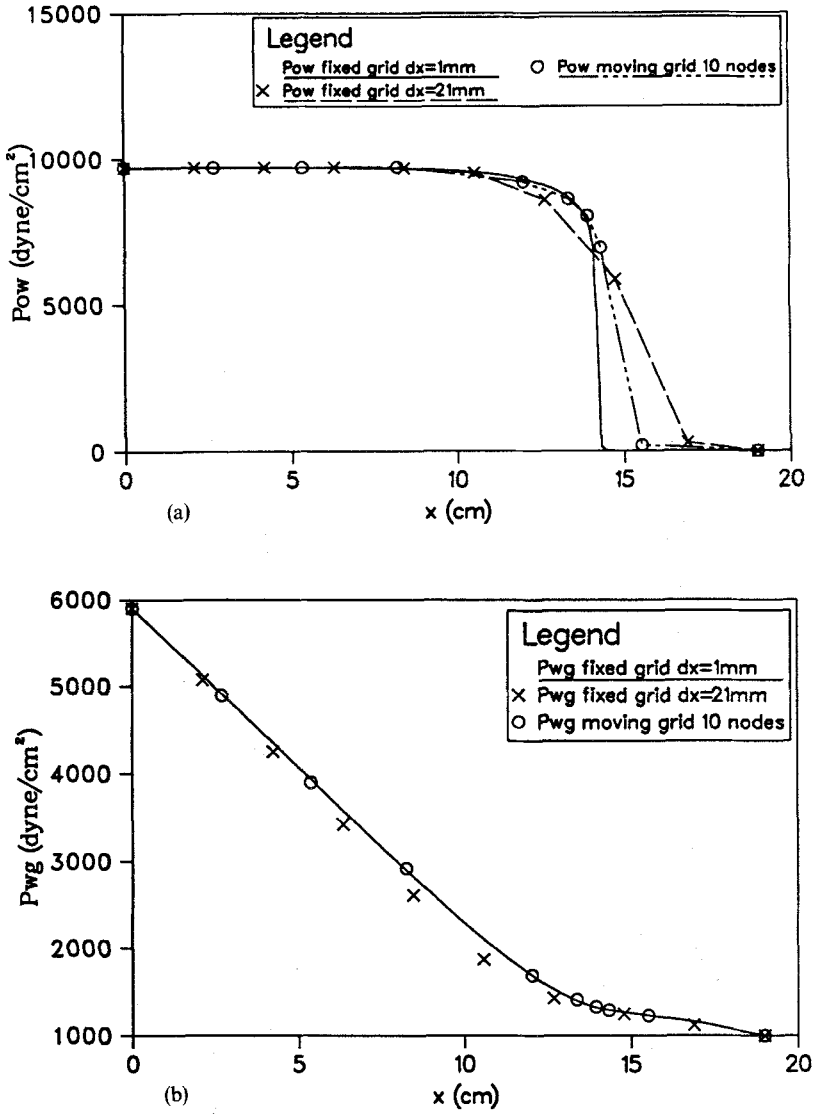

Figure 8. (a) P_{ow} and (b) P_{wg} simulation results of TCE–water horizontal single-front flow after 1000 s

parameters were selected as zero for both ε_1 and ε_2 and $1{\cdot}2 \times 10^{-4}$ and $1{\cdot}0 \times 10^{-4}$ for B_1 and B_2 respectively. Using these parameter values, the MGFEM yields a nodal spacing in the range of a few millimetres about the front between the fluids. This is the nodal spacing that was employed for the very fine fixed grid FEM (FGFEM) computation, which is treated as the 'true solution' for error analysis purposes, as was explained above.

The grid in this problem was updated after a time step in which the largest gradient was located in an element whose length was greater than the smallest element length by some percentage, i.e. when the condition

$$L_i(\max\{P'_j\}) > \min\{L_j\} \times \text{factor}$$

Table III. Comparison between moving and fixed grid FEM

	Fine fixed grid	Coarse fixed grid	Moving grid	Coarse fixed grid (accuracy of moving grid)
No. of nodes	191	10	10	77
Nodal spacing (mm)	1·0	21·1	Changeable	2·4
No. of iterations	22165	3804	1845	20259
CPU time (s)	24991	220	114	2249
Memory space* of constants	128	128	136	128
Memory space of arrays	11600	580	610	9064
Total memory space	11728	708	748	9192
Error†		0·3097	0·06093	0·06094

* Memory space is estimated using double precision for reals and is given in bytes.
† Integration of the first norm of the error over the domain based on the deviation of the organic saturation solution from the fine fixed grid solution. Linear interpolation is used whenever interpolation of the solution is required, and the trapezoidal method is used for integration.

is met. Here $L_i(\max\{P'_j\})$ is the element which contains the maximum gradient, $\min\{L_j\}$ is the smallest element length in the domain and 'factor' is a positive constant greater than 1·0 (the value 1·2 was used in this problem). This front-tracking test was applied in the example simulation because it is very economical, it was known *a priori* that this example problem involved only one front moving in one direction and it provides an adequate grid adaptation frequency. The adaptation frequency is adequate for the simulation example because the centre point of the front requires at least one time step to move from one element to an adjacent element.

Numerical results for this example are shown in Figures 7 and 8. Figure 7 shows the TCE saturation distribution 100, 500 and 1000 s after placing the TCE source at the upstream boundary. Figure 8 shows the solutions for P_{ow} and P_{wg} after 1000 s. In these figures, three numerical solutions are compared. The 'O' symbol represents the nodal locations of the MGFEM and the '×' symbol shows the nodal locations of the coarse FGFEM. Both solutions were obtained with 10 nodes. The solid line shows the 'true solution' which was obtained by employing the fine, 1 mm nodal spacing, FGFEM with 191 nodes. These figures illustrate the concentration of the MGFEM nodes about the organic–water front and the grid adaptivity to the front's motion. The numerical results demonstrate close agreement between the new MGFEM solution and the 'true solution'. In fact, the solution of the MGFEM for S_o deviates from the 'true solution' by only 20% of the deviation of the coarse FGFEM solution (Table III). Here the deviation (error) is the area between the coarse fixed grid solution or the MGFEM organic saturation solution and the fine 'true solution'. The organic saturation solution is used for error calculation because it is the most important variable from the environmental point of view. Errors in P_{ow} and P_{wg} may also be reported, but the error in P_{ow} is related to the error in S_o. This is because S_o is calculated from P_{ow} using (3). The error in P_{wg} is not reported because it is much smaller than the error in P_{ow} (see Figure 7). In addition, it is demonstrated by monitoring the CPU time and calculating the storage requirement (Table III) that, for this simulation, use of the MGFEM resulted in a significant saving of computer resources. The comparison of computer resources is based on the actual CPU time used by the computer and the actual memory space allocated for variable and parameter storage in double precision. The compared CPU time does not include reading of input data, print-out of the input for reference or rearrangement of the data for simulation. This comparison shows that the MGFEM required fewer iterations than the FGFEM for the given example with the same number of nodes and time steps. The reduction in iterations may be due to the greater availability of nodes about the moving front.

A comparison was also made between the moving grid (10 node) and a fixed grid solution of the same accuracy. Here the fixed grid algorithm required 7·7 times the nodes, 5·4 times the memory bytes and 18·8 times the CPU used by the moving grid algorithm. These figures show a significant saving of computer resources by the MGFEM simulator for a one-dimensional two-phase flow problem with a single front (Table III). All computer simulations were performed on Apollo DN4000 computers.

6. CONCLUSIONS

A one-dimensional MGFEM is developed herein to solve the non-linear coupled set of PDEs governing immiscible multiphase flow in porous media. Grid adaptation is based on equi-distribution of the gradient and curvature. The presented moving grid algorithm guarantees a grid-intermingle-free solution for equal upstream and downstream curvature weights. The manner of choosing a representative gradient at each node is discussed in order to facilitate the application of this adaptive grid algorithm to a problem of a coupled set of non-linear PDEs. Also, momentarily fixing the nodes of extremum pressures is considered in order to maintain mass conservation during grid adaptation and to assure the presence of a node at a sink/source point. The model is verified against the Abriola–Pinder[24, 25] FDM model and is applied to a two-phase displacement problem involving TCE and water to illustrate and examine its performance. The MGFEM model exhibited a substantial increase in accuracy over an FGFEM with the same number of degrees of freedom. Further example simulations of this model are given in Part 2 of this paper along with a sensitivity analysis with respect to the moving grid parameters.

ACKNOWLEDGEMENTS

This work was supported in part by grant ECE-8451469 from the National Science Foundation with matching funds from the Electric Power Research Institute under contract RP2377-5. The paper has not been subject to EPRI review and thus the views and opinions expressed herein do not necessary reflect those of EPRI.

APPENDIX: LIST OF SYMBOLS

a_{k_α}	α-phase coefficient in relative permeability equation
a_{s_α}	α-phase coefficient in saturation equation
B_1	upstream curvature weight in nodal distribution
B_2	downstream curvature weight in nodal distribution
g	gravitational acceleration, $[\mathrm{L\,T^{-2}}]$
h_c	capillary head between wetting and non-wetting fluids based on water unit weight, [L]
h_i	length of ith element [L]
kr_α	relative permeability of α-phase
K	intrinsic permeability, $[\mathrm{L^2}]$
K_o	Kkr_o/μ_o, $[\mathrm{L^2}]$
K_w	Kkr_w/μ_w, $[\mathrm{L^2}]$
m_{k_α}	α-phase exponent in relative permeability equation
m_{s_α}	α-phase exponent in saturation equation
n_{k_α}	α-phase exponent in relative permeability equation
n_{s_α}	α-phase exponent in saturation equation
P_c	capillary pressure, $[\mathrm{M\,L^{-1}\,T^{-2}}]$

P_i representative variable at node i
P_i' piecewise linear approximation of representative gradient in ith element
P_α pressure of α-phase, $[M L^{-1} T^{-2}]$
$P_{\alpha\beta}$ capillary pressure between α- and β-phases, $P_{\alpha\beta} = P_\alpha - P_\beta$, $[M L^{-1} T^{-2}]$
$\bar{P}$ average pore fluid pressure, $[M L^{-1} T^{-2}]$
S_α saturation of α-phase
Sr_α residual saturation of α-phase
Ss_α maximum saturation of α-phase
x_i location of ith node, [L]
z length along vertical co-ordinate, [L]

Greek letters

β_s $\beta_\alpha + \beta_\phi$, $[M^{-1} L^4 T^2]$
β_α compressibility of α-phase, $[M^{-1} L^4 T^2]$
β_ϕ compressibility of matrix, $[M^{-1} L^4 T^2]$
γ_o $\rho_o g$, $[M L^{-2} T^{-2}]$
γ_w $\rho_w g$, $[M L^{-2} T^{-2}]$
ε_1 artificial repulsive force
ε_2 artificial viscosity
μ_α dynamic viscosity of α-phase, $[M L^{-1} T^{-1}]$
ρ_α density of α-phase, $[M L^{-3}]$
ϕ matrix porosity

Subscripts

o, w, g denoting organic, water and gas phases respectively

REFERENCES

1. J. F. Thompson, 'A survey of dynamically-adaptive grids in the numerical solution of partial differential equations', *Appl. Numer. Math.*, **1**, 3–27 (1985).
2. R. E. Smith, 'Numerical grid generating techniques', *NASA Conf. Publ. 2166*, 1980.
3. J. F. Thompson, Z. U. A. Warsi and C. W. Mastin, 'Boundary-fitted coordinate systems for numerical solution of partial differential equations—a review', *J. Comput. Phys.*, **47**, 1–108 (1982).
4. J. F. Thompson and Z. U. A. Warsi, 'Three-dimensional grid generation from elliptic systems', *AIAA Paper 83-1905, AIAA Computational Fluid Mechanics Conf.*, Danvers, MA, 1983.
5. J. F. Thompson (ed.), *Numerical Grid Generation*, North-Holland, Amsterdam, 1982.
6. J. F. Thompson, 'Grid generation techniques in computational fluid dynamics', *AIAA J.*, **22**(11), 1505–1523 (1984).
7. J. Douglas Jr., D. L. Darlow, M. F. Wheeler and R. D. Kendal, 'Self adaptive finite element and finite difference methods for one-dimensional two-phase immiscible flow', *Comp. Methods Appl. Mech. Eng.*, **47**, 119–130 (1984).
8. R. J. Gelinas, S. K. Doss and K. Miller, 'The moving finite element method: application to general partial differential equation with large gradients', *J. Comput. Phys.*, **40**, 202–249 (1981).
9. F. G. Gruham, A. Mueller, K. Sepehrnoori and R. L. Thrasher, 'Moving elements for transport processes', *SPE Reservoir Eng.*, **2**, 401–408 (1987).
10. O. K. Jensen and B. A. Finlayson, 'Solution of transport equations using a moving coordinate system', *Adv. Water Resources*, **3**, 9–18 (1980).
11. K. Miller and R. Miller, 'Moving finite elements. I', *SIAM J. Numer. Anal.*, **18**, 1019–1032 (1981).
12. G. H. Schmidt and F. J. Jacobs, 'Adaptive local grid refinement and multi-grid in numerical reservoir simulation', *J. Comput. Phys.*, **77**, 140–165 (1988).
13. S. Adjerid and J. E. Flaherty, 'A moving mesh finite element method with local refinement for parabolic partial differential equations', *Comput. Methods Appl. Mech. Eng.*, **55**, 3–26 (1986).
14. R. Miller, 'Moving Finite Elements. II', *SIAM J. Numer. Anal.*, **18**, 1033–1057 (1981).

15. R. Löhner, 'An adaptive finite element scheme for transient problems in CFD', *Comput. Methods Appl. Mech. Eng.*, **61**, 323–338 (1987).
16. C. M. Mosher, 'A variable node finite element method', *J. Comput. Phys.*, **57**, 157–187 (1985).
17. J. K. Dukowicz, 'A simplified adaptive mesh technique derived from moving finite element method', *J. Comput. Phys.*, **56**, 324–342 (1984).
18. M. Th. van Genuchten, 'Closed-form equation for predicting the hydraulic conductivity of unsaturated soil', *Soil Sci. Soc. Am. J.*, **44**, 892–898 (1980).
19. Y. Mualem, 'A new model for predicting hydraulic conductivity of unsaturated porous media', *Water Resources Res.*, **12**, 513–522 (1976).
20. L. M. Abriola, '*Multiphase Migration of Organic Compounds in Porous Medium, a Mathematical Model*, Springer, Berlin, 1984.
21. G. F. Pinder and L. M. Abriola, 'On simulation of nonaqueous phase organic compounds in the subsurface', *Water Resources Res.*, **22**, 109S–119S (1986).
22. J. C. Parker, R. J. Lenhard and T. Kuppusamy, 'A parametric model for constitutive properties governing multiphase fluid conduction in porous media', *Water Resources Res.*, **23**, 618–624 (1987).
23. H. L. Stone, 'Probability model for estimating three-phase relative permeability', *J. Petrol. Technol.*, **22**, 214–218 (1970).
24. L. M. Abriola and G. F. Pinder, 'A multiphase approach to the modeling of porous media contamination by organic compounds: 1. Equation development', *Water Resources Res.*, **21**, 11–18 (1985).
25. L. M. Abriola and G. F. Pinder, 'A multiphase approach to the modeling of porous media contamination by organic compounds: 2. Numerical simulation', *Water Resources Res.*, **21**, 19–26 (1985).
26. C. R. Faust, 'Transport of immiscible fluids within and below the unsaturated zone: a numerical model', *Water Resources Res.*, **21**, 587–596 (1985).
27. T. Kuppusamy, J. Sheng, J. C. Parker and R. J. Lenhard, 'Finite-element analysis of multiphase immiscible flow through soils', *Water Resources Res.*, **23**, 625–631 (1987).
28. R. E. Benner Jr., H. T. Davis and L. E. Scriven, 'Adaptive zoning for singular problems in two dimensions', *J. Comput. Phys.*, **63**, 529–549 (1987).
29. J. G. Bloom, J. M. Sanz-Serna and J. G. Verwer, 'On simple moving grid methods for one-dimensional evolutionary partial differential equations', *J. Comput. Phys.*, **74**, 191–213 (1988).
30. A. Berman and R. R. Plemons, *Nonnegative Matrices in the Mathematical Sciences*, Academic, New York, 1979.
31. M. Fiedler and R. R. Patāk, 'On the matrices with nonpositive off-diagonal elements and positive principal minors', *Czech. Math. J.*, **12**, 382–400 (1962).
32. L. M. Aziz and A. Settari, *Petroleum Reservoir Simulation*, Applied Science, London, 1979.
33. A. Gamliel, 'Simulation of immiscible multiphase flow in porous media using a moving grid finite element method', *Ph.D. Thesis*, Department of Civil Engineering, The University of Michigan, 1989.